Smart Structures and Systems, *Vol. 16, No. 4 (2015) 701-723*
DOI: http://dx.doi.org/10.12989/sss.2015.16.4.701

Comparison of seismic behavior of long period SDOF systems mounted on friction isolators under near-field earthquakes

Vahid Loghman* and Faramarz Khoshnoudian[a]

Faculty of Civil Engineering, AmirKabir University of Technology (Tehran Polytechnic), Hafez St., Tehran, Iran

(Received February 15, 2015, Revised April 26, 2015, Accepted May 3, 2015)

Abstract. Friction isolators are one of the most important types of bearings used to mitigate damages of earthquakes. The adaptive behavior of these isolators allows them to achieve multiple levels of performances and predictable seismic behavior during different earthquake hazard levels. There are three main types of friction isolators. The first generation with one sliding surface is known as Friction Pendulum System (FPS) isolators. The double concave friction pendulum (DCFP) with two sliding surfaces is an advanced form of FPS, and the third one, with fully adaptive behavior, is named as triple concave friction pendulum (TCFP). The current study has been conducted to investigate and compare seismic responses of these three types of isolators. The structure is idealized as a two-dimensional single degree of freedom (SDOF) resting on isolators. The coupled differential equations of motion are derived and solved using state space formulation. Seismic responses of isolated structures using each one of these isolators are investigated under seven near fault earthquake motions. The peak values of bearing displacement and base shear are studied employing the variation of essential parameters such as superstructure period, effective isolation period and effective damping of isolator. The results demonstrate a more efficient seismic behavior of TCFP isolator comparing to the other types of isolators. This efficiency depends on the selected effective isolation period as well as effective isolation damping. The investigation shows that increasing the effective isolation period or decreasing the effective isolation damping improves the seismic behavior of TCFP compared to the other isolators. The maximum difference in seismic responses, the base shear and the bearing displacement, for the TCFP isolator are calculated 26.8 and 13.4 percent less than the DCFP and FPS in effective isolation damping equal to 10%, respectively.

Keywords: friction isolators; friction pendulum system; double concave friction pendulum; triple concave friction pendulum; seismic responses; near fault ground motions

1. Introduction

The concept of employing base isolation system in buildings is not new. The first suggested idea for using the isolation system was published by Touaillon in 1870 which employed mechanical equipment to separate a building from strong ground motions. It is noted that the main concept has not been changed since the idea was introduced, but the capability of using this technology to obtain predictable and reliable behavior has been improved (Fenz and Constantinou

*Corresponding author, Msc Graduated, E-mail: vahid.loghman@aut.ac.ir
[a] Professor, E-mail: khoshnud@aut.ac.ir

http://www.techno-press.org/?journal=sss&subpage=8 ISSN: 1738-1584 (Print), 1738-1991 (Online)

2008a).

Generally, seismic isolators provide flexibility and energy dissipation to protect the superstructure from damages during extreme ground excitations. Many mechanisms have been invented and introduced to allow for such isolation. One of the most applicable isolation systems, known as sliding bearings, exploits friction as a main implement. Pure-friction (P-F) system is the simplest sliding system device which does not have any restoring force (Mostaghel and Tanbakuchi 1983, Yang *et al.* 1990). The main problem of the P-F systems is the large sliding and residual displacement in strong motions due to the lack of restoring force.

Sliding systems such as the resilient-friction base isolator (R-FBI) system (Mostaghel and Khodaverdian 1987); the friction pendulum system (FPS) (Zayas *et al.* 1987, 1990), the Electricite de France (EDF) system (Gueraud *et al.* 1985), and the variable friction pendulum system (VFPS) (Panchal and Jangid 2008) were invented to solve the inherent problem of the P-F systems and improve the seismic behavior.

Using surface curvature to provide the restoring force is one of the applicable ideas to elucidate the latter problem. According to this concept, a friction pendulum system (FPS) was introduced to create a restoring force from the pendulum action of the weight of the structure (Fig. 1(a)). Zayas *et al.* (1987, 1990) demonstrated that the natural period of this system becomes independent of the mass and stiffness of the superstructure, as it only depends on the radius of the sliding surface. They also initiated and formulated the FPS behavior. Almazan *et al.* (1998) investigated the seismic responses of SDOF and MDOF structures mounted on FPS isolators considering different aspects, subjected to three components of earthquake. Rabiei and Khoshnoudian (2011) also studied the seismic responses of multi-storey friction pendulum base isolated structures taking vertical component of earthquakes into account where the considerable effects of the vertical component of earthquake on seismic responses of isolated structures mounted on FPS bearings were demonstrated.

To optimize the FPS seismic behavior and enhance the capacity of bearing displacement, two sliding surfaces were employed on the top and the bottom of the isolator. This system was introduced as the double concave friction pendulum (DCFP), as illustrated in Fig. 1(b). Using two sliding surfaces gives the advantage of double displacement bearing capacity in comparison with similar FPS systems. Also, employing two sliding surfaces can give tri-linear behavior if top and bottom plates have different coefficients of friction which cause a different behavior from the FPS isolators. Theoretical modeling of DCFPs has been studied by Tsai *et al.* (2004, 2005) and Fenz and Constantinou (2006). Kim and Yun (2007) studied the benefits of tri-linear DCFP over the bi-linear DCFP for isolating bridges from strong ground motions. They concluded that tri-linear DCFP reduces the base shear of the pier in the range of 15%~40% more than bi-linear DCFP. Influence of isolator characteristics on the responses of base-isolated structures was investigated by Matsagar and Jangid (2004). They considered different mathematical models depicted by bi-linear hysteretic and equivalent linear elastic–viscous behaviors. It was noted that the responses of base-isolated structures are significantly affected by the shape of hysteresis behavior of the isolator. Khoshnoudian and Hemmati (2011) investigated seismic responses of base-isolated structures using DCFP with tri-linear and bi-linear behaviors for a SDOF structure. It was demonstrated that the tri-linear DCFP bearings, in comparison with bi-linear ones, can decrease the base shear up to 48%. However, displacements of the sliding surfaces resulted from tri-linear DCEP bearings are 57% larger than those obtained from the bi-linear systems. Khoshnoudian and Rabiei (2010) studied the effect of the vertical component of earthquakes on the seismic responses of DCFP base-isolated structures. It was noted that by overlooking the effect of the vertical

component of earthquake, the seismic responses such as bearing displacement and base shear are estimated less than their real values. This error is calculated about 5 and 22 percent for bearing displacement as well as base shear, respectively. Bagheri and Khoshnoudian (2014) investigated the effect of impact with adjacent structures for base-isolated structures mounted on DCFP isolators.

The triple concave friction pendulum (TCFP) is the third generation of this type of isolation systems. The TCFP system consists of four concave surfaces and three independent mechanisms (Fig. 1(c)). By choosing an appropriate configuration, this system can vary its stiffness and damping during different seismic hazard levels. This ability allows it an adaptive seismic behavior under different levels of earthquake shaking (Fenz and Constantinou 2007a). The analytical behavior of TCFP, including a suitable cyclic model with experimental verification has been reported by Fenz and Constantinou (2007 a,b and 2008a) and by Morgan and Mahin (2011). Fenz and Constantinou (2008 b,c) introduced a series model which consists of three FPS isolator connected in series. Fadi and Constantinou (2009) evaluated simplified methods of analysis for isolated structures using TCFP isolator. They used a SDOF system with linear stiffness and viscous damping. They concluded that simplified methods of analysis provide acceptable and often conservative isolator displacement and underestimates the peak velocity by approximately 35%. Reliable performance of TCFP has been demonstrated by Morgan and Mahin (2011) in comparison with other devices with bilinear behavior like FPS. The bi-directional behavior of TCFP has been studied and examined by Becker and Mahin (2011). Loghman, Khosnoudian and Banazadeh (2013) investigated the effect of vertical component of earthquake on seismic responses of base-isolated structures mounted on TCFP bearings.

Although seismic behavior of following isolators: FPS, DCFP and TCFP bearings, has been developed in recent years, e.g., Malekzadeh and Taghikhany (2010), Panchal and Jangid (2011), Tajammolian *et al*. (2014), a complete investigation to compare the seismic responses of isolated structures using these isolators has not been conducted yet. Therefore, the present research is performed to compare the seismic behavior of base-isolated structures mounted on three generations of sliding bearings. Comparison is accomplished for base shear and bearing displacement as the main structure responses subjected to seven near field ground motions. Also, the influences of superstructure period, effective isolation period, and effective isolation damping have been considered in this investigation.

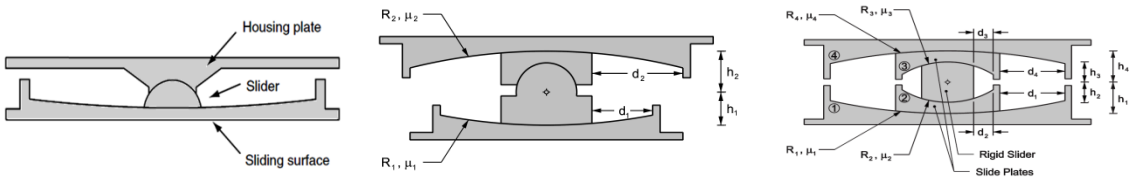

(a) (b) (c)

Fig. 1 Cross section of: (a) FPS (b) DCFP and (c) TCFP bearings (Fenz and Constantinou 2008c)

2. Seismic behavior and mathematical modeling of TCFP and DCFP isolators

Fig. 2 illustrates the seismic behavior of different friction isolation systems. The hysteresis curve of FPS isolators is shown in Fig. 2(a). The DCFP isolators due to its friction properties values of top and bottom sliding surfaces can provide two types of hysteresis loops. The DCFP isolator with the equal coefficient of friction in top and bottom surfaces behave like a FPS isolator and experience a bi-linear hysteresis (Fig. 2(a)), while selecting different coefficient of friction for top and bottom surfaces changes the behavior to a tri-linear hysteresis curve (Fig. 2(b)). The TCFP isolation system has more intricate and complicated hysteresis behavior. A TCFP with fully adaptive behavior can experience 5 regimes of movement. This happens when the coefficient of friction of the top and bottom surfaces (Fig. 1(c)) select in which $\mu_2=\mu_3<\mu_1<\mu_4$. These regimes are shown in Fig. 2(c). The main difference in hysteresis behavior of a TCFP isolator and a DCFP with tri-linear is in IV and V regimes of movements in which the TCFP experiences stiffening sections.

Furthermore, TCFP isolators provide their displacement capacity through four surfaces. This fact supplies more small dimensions in comparison to the other types with the same displacement capacity. Also, DCFP can provide the capacity in two sliding surfaces which means that it has smaller size in comparison to FPS with the same displacement capacity.

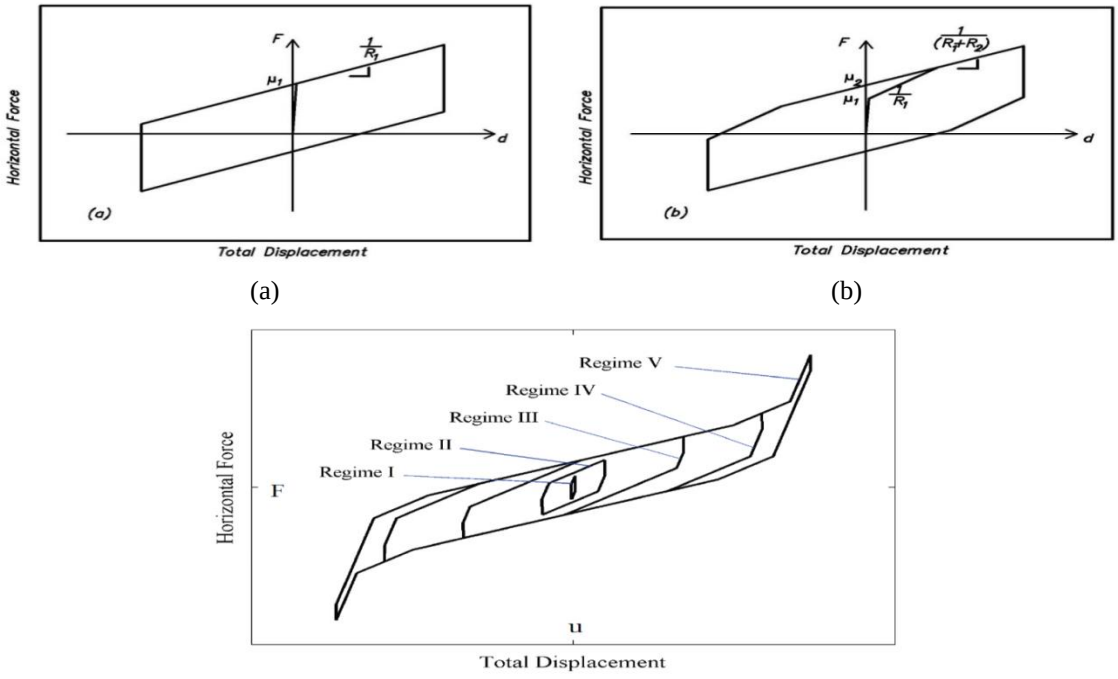

Fig. 2 Hysteresis behavior of: (a) FPS (b) DCFP, Hysteresis behavior of: (c) TCFP bearings (Constantinou *et al*. (2011))

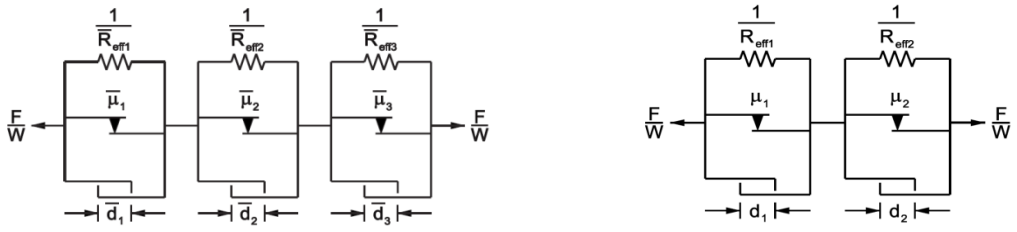

Fig. 3 Series model with FP elements for (a) TCFP and (b) DCFP (Fenz and Constantinou 2008c)

Two approaches to model multi-spherical sliding bearing were introduced by Fenz and Constantinou (2008c): develop and implement a new hysteresis rule to trace the overall behavior, or combine existing nonlinear elements in such a way that the overall behavior is captured. The latter approach uses three FPS elements and two FPS elements connected in series to idealize TCFP and DCFP isolators, respectively. Then the governing equations for these bearings are based on friction pendulum bearings equations of motion. Fig. 3 shows the series elements for TCFP as well as DCFP which consist of parallel arrangements of (a) a linear spring, (b) a velocity-dependent perfectly plastic friction element, and (c) a gap element.

The TCFP consists of four sliding surfaces as it is shown in Fig. 1(c). Due to similar physical and geometrical properties of inner sliding surfaces (2 and 3), they make one independent element. Fenz and Constantinou (2008 b,c) demonstrated that the revised properties in which the TCFP is modeled by three independent FPS elements connected in series.

The parameters of series elements employing to model TCFP isolators are represented in Table 1. In this table, μ_i is the coefficient of friction of surface i, R_{effi} stands for the radius of curvature of the sliding surface i, d_i represents the displacement capacity of surface i and a_i is the rate parameter that controls the variation of the coefficient of friction with sliding velocity.

Based on the equation for a FPS isolator the horizontal force Fi in the isolator can be written as

$$F_i = \frac{W}{R_{effi}} u_i + \mu_i W \; Z_i + F_{ri} \tag{1}$$

Table 1 Parameters of series model of the TCFP bearing (Fenz and Constantinou 2008c)

	Coefficients of friction	Radii of curvature	Nominal displacement capacity	Rate parameter
Element 1	$\bar{\mu}_1 = \mu_2 = \mu_3$	$\bar{R}_{eff\,1} = R_{eff\,2} + R_{eff\,3}$	$\bar{d}_1 = d_{tot} - \left(\bar{d}_2 + \bar{d}_3\right)$	$\bar{a}_1 = \frac{1}{2}\frac{\left(a_2 + a_3\right)}{2}$
Element 2	$\bar{\mu}_2 = \mu_1$	$\bar{R}_{eff\,2} = R_{eff\,1} - R_{eff\,2}$	$\bar{d}_2 = \frac{R_{eff\,1} - R_{eff\,2}}{R_{eff\,1}} d_1$	$\bar{a}_2 = \frac{R_{eff\,1}}{R_{eff\,1} - R_{eff\,2}} a_1$
Element 3	$\bar{\mu}_3 = \mu_4$	$\bar{R}_{eff\,3} = R_{eff\,4} - R_{eff\,3}$	$\bar{d}_3 = \frac{R_{eff\,4} - R_{eff\,3}}{R_{eff\,4}} d_4$	$\bar{a}_3 = \frac{R_{eff\,4}}{R_{eff\,4} - R_{eff\,3}} a_4$

u_i : the bearing displacement, W: the weight of structure, R_{effi}: the radius of curvature of the sliding surface, μ_i: the coefficient of friction, Z_i: a dimensionless hysteretic variable defined in Eq. (2), and F_{ri}: the contact effect with restrainers identified in Eq. (3).

$$\frac{dZ_i}{dt} = \frac{1}{u_{yi}} \left\{ A_i - \left|Z_i\right|^{\eta_i} \left[\gamma_i \, sign(\dot{u}_i Z_i) + \beta_i\right] \right\} \dot{u}_i \tag{2}$$

Where u_{yi} is the yield displacement, $\dot{u}_i$ is the sliding velocity, and $A_i, \eta_i, \gamma_i, \beta_i$ are dimensionless quantities that control the shape of the hysteresis loop.

$$F_{ri} = k_{ri}(\left|u_i\right| - d_i) sign(u_i) H\left(\left|u_i\right| - d_i\right) \tag{3}$$

k_{ri} is the stiffness after contacting the displacement restrainers which is assigned a large value, and H is the Heaviside function.

3. TCFP, DCFP and FPS isolators design

To design isolators, it is important to choose proper parameters to estimate the overall behavior. Seismic codes usually use effective period (T_{eff}) and effective damping (ξ_{eff}) as designing parameters of isolated structures. These can be expressed by the following equations

$$T_{eff} = 2\pi \sqrt{\frac{W}{K_{eff}\, g}} \quad , \xi_{eff} = \frac{1}{2\pi}\left[\frac{E_{loop}}{K_{eff}\, D^2}\right] \tag{4}$$

In which E_{loop} is the energy dissipated in each cycle of the isolator hysteresis loop, K_{eff} is the effective linear stiffness and D is the target displacement of the isolator.

In this study, to compare the seismic behavior of isolators, displacement in the end of sliding regime IV or beginning of sliding regime V for TCFP has been chosen as a target displacement, until the whole sliding regime of TCFP is covered. Due to this assumption, comparison must be performed in maximum considered earthquake (MCE) level.

Fig. 4 shows the force-displacement relation for an isolator system with bilinear hysteretic behavior. In this system, Q_d is the characteristic strength, K_d stands for the post-elastic stiffness and Y is the yield displacement of the system. In this system, E_{loop} and K_{eff} are defined by the following equations (Constantinou *et al*. 2011)

$$E_{loop} = 4Q_d \left(D - Y\right) \tag{5}$$

$$K_{eff} = K_d + \frac{Q_d}{D} \tag{6}$$

Q_d and K_d would be μW and W/R for a FPS system, respectively. The yield displacement Y has been suggested to assume a value of 0.01 inch by Scheller and Constantinou (1999), but the Y parameter has not been considered in this research. According to these assumptions K_{eff} and E_{loop}

are derived as

$$K_{eff} = \left(\frac{\mu}{D} + \frac{1}{R} \right) W \tag{7}$$

$$E_{loop} = 4 \mu D W \tag{8}$$

For a DCFP isolation system, in sliding regime II (Fenz and Constantinou (2008 a,c)), these equations would change to Eqs. (9)-(11) where u^* is the isolator displacement at the end of sliding regime I. Fig. 5 illustrates the force-displacement relation for a DCFP system.

$$K_{eff} = \left(\mu_2 + \frac{\left(D - u^* \right)}{R_{eff\,1} + R_{eff\,2}} \right) \frac{W}{D} \tag{9}$$

$$E_{loop} = 4 \left(\mu_2 - \frac{1}{R_{eff\,1} + R_{eff\,2}} u^* \right) DW - 4 \left(\frac{1}{R_{eff\,1}} - \frac{1}{R_{eff\,1} + R_{eff\,2}} \right) u^{*2} W \tag{10}$$

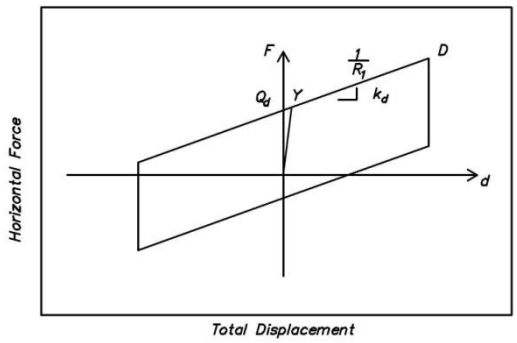

Fig. 4 Idealized force-displacement of typical seismic isolation system

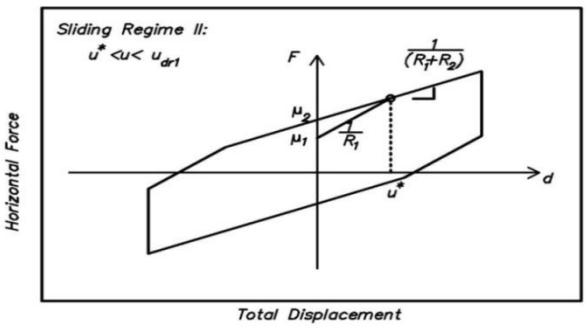

Fig. 5 Force-displacement relation for DCFP system

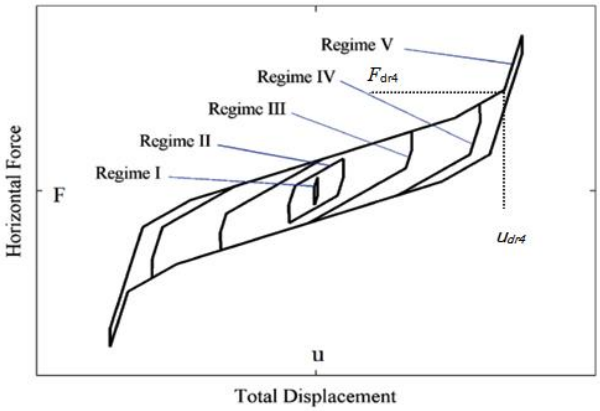

Fig. 6 Force-displacement relation for TCFP isolator (Constantinou *et al*. 2011)

$$u^{*} = \left(\mu_2 - \mu_1\right) R_{eff\,1} \tag{11}$$

In sliding regime IV, these equations would change to the following equations for a TCFP isolation system (Fenz and Constantinou 2008 a,c), (Fig. 6).

$$K_{eff} = \frac{F_{dr\,4}}{u_{dr\,4}} \tag{12}$$

$$F_{dr\,4} = \frac{W}{R_{eff\,4}} d_4 + F_{f\,4} \tag{13}$$

Where u_{dr4} depends on the previous sliding regime displacements and u^{*}, u^{**} and u_{dr1} are the isolator displacement at the end of sliding regimes I, II, and III, respectively (Fenz and Constantinou (2008 a,c)).

$$u_{dr\,4} = u_{dr1} + \left[\left(\frac{d_4}{R_{eff\,4}} + \mu_4\right) - \left(\frac{d_1}{R_{eff\,1}} + \mu_1\right)\right]\left(R_{eff\,2} + R_{eff\,4}\right) \tag{14}$$

$$u_{dr1} = u^{**} + d_1\left(1 + \frac{R_{eff\,4}}{R_{eff\,1}}\right) - \left(\mu_4 - \mu_1\right)\left(R_{eff\,4} + R_{eff\,1}\right) \tag{15}$$

$$u^{**} = u^{*} + \left(\mu_4 - \mu_1\right)\left(R_{eff\,1} + R_{eff\,3}\right) \tag{16}$$

$$u^{*} = \left(\mu_1 - \mu_2\right) R_{eff\,2} + \left(\mu_1 - \mu_3\right) R_{eff\,3} \tag{17}$$

E_{loop} stands for the energy dissipated in each cycle of isolator that can obtain from following equation.

$$E_{loop} = 4\left(\mu_1 + \frac{d_1}{R_{eff\,1}} - \frac{1}{R_{eff\,1}+R_{eff\,2}}u_{dr1}\right)u_{dr4}W - 4\left(\frac{1}{R_{eff\,1}+R_{eff\,4}} - \frac{1}{R_{eff\,1}+R_{eff\,2}}\right)u_{dr1}{}^2 W$$
$$-4\left(\frac{1}{R_{eff\,1}+R_{eff\,2}} - \frac{1}{R_{eff\,1}+R_{eff\,4}}\right)u^{**2}W - 4\left(\frac{1}{R_{eff\,2}+R_{eff\,3}} - \frac{1}{R_{eff\,1}+R_{eff\,2}}\right)u^{*2}W \quad (18)$$

Then, to compare the seismic responses, the isolator parameters have been chosen to make the same effective period and damping. The configurations for the three types of isolation systems with different isolation periods and ξ_{eff}=15% are listed in Tables 2-4.

Table 2 Characteristics of FPS isolators

Design	Displacement Capacity d (m)	Effective Radii R_{eff} (m)	Friction Coefficient μ
FPS-5-15	1	8.15	0.037
FPS-4-15	1	5.25	0.056
FPS-3-15	1	3	0.10

Table 3 Characteristics of DCFP isolators

Design	Displacement Capacity		Effective Radii		Friction Coefficient	
	d_1 (m)	d_2 (m)	R_{eff1} (m)	R_{eff2} (m)	μ_1	μ_2
DCFP-5-15	0.5	0.5	5.6	2.8	0.025	0.07
DCFP-4-15	0.5	0.5	3.6	1.8	0.04	0.11
DCFP-3-15	0.5	0.5	2	1	0.09	0.13

Table 4 Characteristics of TCFP isolators

Design	Displacement Capacity (m)			Effective Radii		Friction Coefficient		
	d_1= d_4	d_2= d_3	d (total)	R_{eff1}=R_{eff4}	R_{eff2}=R_{eff3}	μ_2=μ_3	μ_1	μ_4
TCFP-5-15	0.45	0.05	1	5.5	0.45	0.02	0.038	0.07
TCFP-4-15	0.45	0.05	1	3.5	0.3	0.02	0.06	0.11
TCFP-3-15	0.45	0.05	1	2	0.3	0.05	0.115	0.2

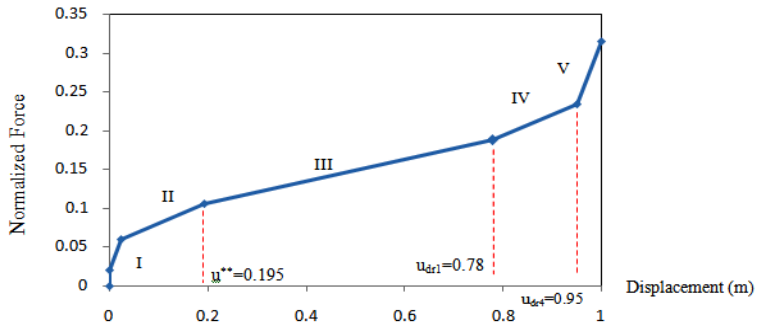

Fig. 7 Force-displacement for TCFP isolator with T_{eff}=4 s and ξ_{eff}=15%

According to this assumption, for T_{eff}=4 s, the target displacement D is equal to u_{dr4} = 0.95 m. The important point is that the configuration which is due to selected effective period and damping in target displacement is not unique, thus selecting the appropriate parameters for isolation system is very important. As shown in Fig. 2, the main difference in the hysteretic diagram of TCFP and other isolation system is the stiffening sliding regimes that happened in parts IV and V of the hysteretic diagram. Therefore, the proportions of parts IV and V of the force-displacement diagram in the hysteretic behavior of TCFP system play an important role to differentiate the seismic responses from other isolation systems like FPS as well as DCFP. In this research, the TCFP configuration was adjusted to limit the regimes IV and V about to 25% of the TCFP backbone curve. It is predicted that the results will change if the proportions of different sliding regimes alter, even if the new configuration meet the same effective period and damping. These properties are chosen by trial and error and these may not the optimal values. Also, as a matter of fact these are not standard sizes and values from manufacturers.

As an example Fig. 7 shows the monotonic TCFP backbone curve for T_{eff}=4 s and ξ_{eff}=15%. In this figure, the isolator displacement at the end of every sliding regime is illustrated.

4. Modeling of base-isolated structure

Fig. 8 represents the assumed structural system, which is an idealized two-dimensional single-story building model, mounted on a TCFP, DCFP or FPS bearings. The top mass m_s and the base mass m_b are rigid decks supported on mass-less columns. The superstructure is assumed to be linear elastic. This is a reasonable assumption, since the purpose of the base isolation is to reduce the earthquake forces on the structure. The center of mass (CM) of the top deck and the base deck are assumed to be vertically aligned. As a result, there is no torsional coupling.

The dynamic behavior of the investigated system subjected to earthquake excitation can be described by the following four degrees of freedom: u_{xs} and u_{zs} which are the displacement of the superstructure at the center of the top deck relative to the base deck in the x and the z directions, respectively, u_{xb} and u_{zb} which stand for the base displacement at the center of the base deck relative to the ground in the x and the z directions, respectively. The equation of motion for the structure in the vertical direction can be expressed in matrix form as

$$\begin{bmatrix} m_s & m_s \\ 0 & m_b \end{bmatrix}\begin{bmatrix} \ddot{u}_{zs} \\ \ddot{u}_{zg} \end{bmatrix}+\begin{bmatrix} c_z & 0 \\ -c_z & 0 \end{bmatrix}\begin{bmatrix} \dot{u}_{zs} \\ \dot{u}_{zg} \end{bmatrix}+\begin{bmatrix} k_z & 0 \\ -k_z & 0 \end{bmatrix}\begin{bmatrix} u_{zs} \\ u_{zg} \end{bmatrix}=\begin{bmatrix} -w_s \\ N-w_b \end{bmatrix} \tag{19}$$

Where w_s is the weight of the superstructure deck and w_b is the weight of the base deck, u_{zg} , $\dot{u}_{zg}$ and $\ddot{u}_{zg}$ are displacement, velocity and acceleration of the ground in the vertical direction, in the same order. k_z and c_z are vertical stiffness and damping, represented by

$$k_z = \beta^2 k_x \quad and \quad C_z = \beta\, C_x \tag{20}$$

where β represents the ratio of vertical to horizontal vibration frequency of the structure. Typical values for β in frame buildings range between 5 and 15 and β=7 is selected for the present study (Almazan *et al.* 1998). Based on the mathematical model of TCFP and DCFP bearings, equations of motion for series FP elements that attached to a SDOF superstructure were formulated using the state-space approach and computer programs were written in Matlab using the Ode15s solver to investigate the seismic responses of isolated structures employing these different isolators. The results obtained through this program are discussed.

5. Verification of written computer program

To verify the accuracy of the written computer programs the analysis outputs were compared with the results obtained from different sources. The TCFP code verified with previous investigations written by Fenz and Constantinou (2008 b,c). In that study the responses of the TCFP base-isolated structure were studied subjected to the Elcentro 1940 excitation multiplied by a scaling factor of 2.15. The structural model was a 2D single story building, similar to that presented in Fig. 8, resting on a TCFP bearing. Properties proposed by Fenz and Constantinou (2008 b,c) were used. Accordingly, the following parameters are used:

ξ=0.25%, T_s=0.2 sec, m_b/m_s=0.5, A_i=1, β_i=0.1, η_i=2, γ_i=0.9, u_{yi}=0.01 cm. Properties of series element are shown in Table 5.

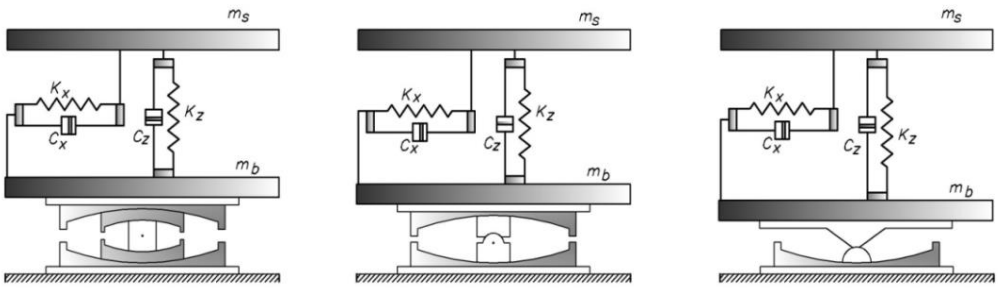

Fig. 8 Idealized two-dimensional single-story structure resting on TCFP, DCFP & FPS bearings

Table 5 Parameters of series model of the triple FP bearing Fenz and Constantinou (2008c)

	Coefficients of friction	Radii of curvature	Nominal displacement capacity	Rate parameter
Element 1	$\bar{\mu}_1 = 0.01 - 0.02$	$\bar{R}_{eff\ 1} = 106\,mm$	$\bar{d}_1 = -$	$\bar{a}_1 = 0.05\ sec/mm$
Element 2	$\bar{\mu}_2 = 0.02 - 0.04$	$\bar{R}_{eff\ 2} = 382\,mm$	$\bar{d}_2 = 56.2\,mm$	$\bar{a}_2 = 0.11\ sec/mm$
Element 3	$\bar{\mu}_3 = 0.06 - 0.13$	$\bar{R}_{eff\ 3} = 382\,mm$	$\bar{d}_3 = 56.2\,mm$	$\bar{a}_3 = 0.11\ sec/mm$

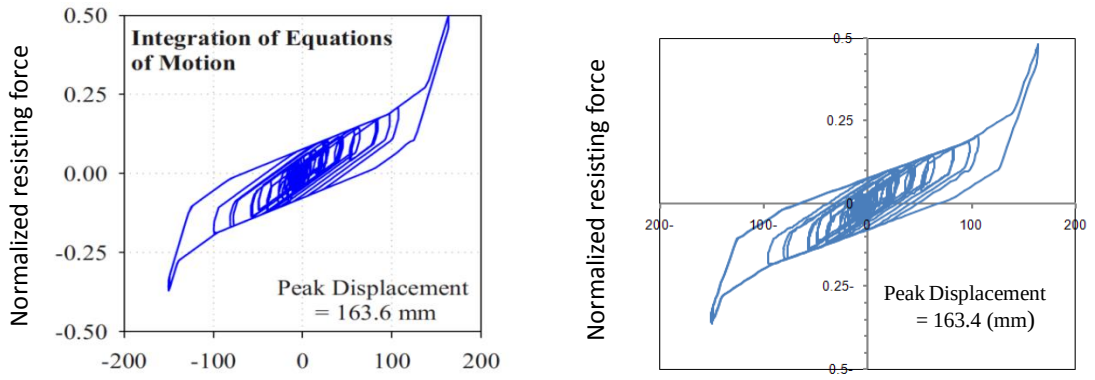

(a) Fenz and Constantinou investigation (2008c) (b) Written Matlab program

Fig. 9 Comparison of Hysteretic diagrams

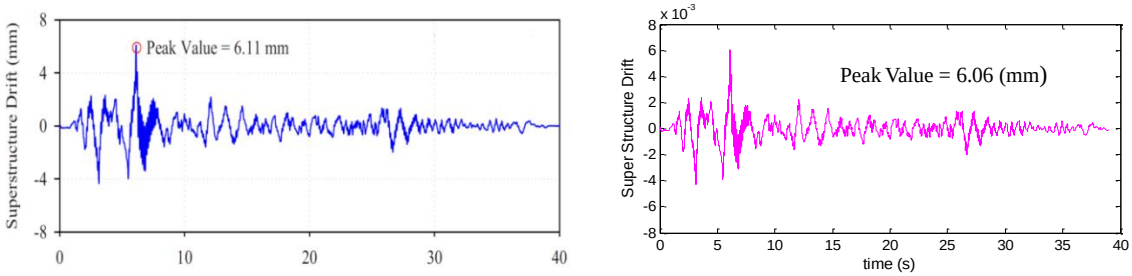

(a) Fenz and Constantinou investigation (2008c) (b) Written Matlab program

Fig. 10 Comparison of superstructure drift

The hysteretic diagram obtained from the Matlab code and that obtained in the previous investigation (Fenz and Constantinou 2008 b,c) are compared in Fig. 9. The similarities between these diagrams clearly confirm the accuracy of the developed program. In these diagrams, the resisting force is normalized by the superstructure weight.

In addition, the comparison of time history superstructure drift confirms the reliability of the developed program (Fig. 10).

Also, the results of DCFP and FPS codes were compared and verified with the previous investigations written by Fenz and Constantinou (2008a), Matsagar and Jangid (2004).

6. Numerical study

The responses of a two-dimensional SDOF building resting on different types of friction concave bearings subjected to two components of earthquake excitations were investigated. The responses of the isolated structures considered herein are the base shear of the superstructure and the relative bearing displacement, because the base shear is an index of the exerted forces on the structure due to the earthquake excitation and the latter is a measure of displacement between the isolated structure and the ground, which is a crucial parameter in design of isolators. The damping ratio of the superstructure is assumed to be 2%. In the present study, the mass ratio m_b/m_s is assumed to be constant and the dimensionless quantities that control the shape of the hysteresis loop were set as in the previous investigation conducted by Fenz and Constantinou (2008c). To compare the time history of displacement for the different types of isolators, the capacity of gap elements in the last sliding regime for each isolation system (e.g., element 1 which shows the capacity for inner surfaces for TCFP in Table 5 were set to large enough values so that they can slide without reaching the isolator restrainers. Seven near field earthquake records were considered and applied to the isolated structure. The characteristics of these records are shown in Table 6.

These earthquakes were selected due to their considerable vertical components as well as their remarkable range of pulse period, as demonstrated by wavelet analysis classification of the records (Baker 2007). These records are categorized by FEMA 695 in the near field pulse record subset To consider and compare the whole sliding regime of TCFP isolator with other isolation systems, it was necessary that the TCFP system experienced all sliding regimes.

Table 6 Characteristics of earthquake records

Item	Earthquake Record	Station	Peak acceleration in Horizontal direction(g)	Peak acceleration in Vertical direction(g)	Pulse Period (sec)	Magnitude
1	Kobe 1995	Takatori	0.616	0.27	1.6	6.9
2	Northridge 1994	Sylmar	0.843	0.535	3.1	6.7
3	Imperial Valley-06 1979	Elcentro #7	0.46	0.54	4.2	6.5
4	Loma Prieta 1989	Saratoga	0.52	0.38	4.5	6.9
5	Landers 1992	Lucerne	0.79	0.82	5.1	7.3
6	Duzce 1999	Duzce	0.535	0.36	5.6	7.1
7	ChiChi 1999	TCU065	0.82	0.27	5.7	7.6

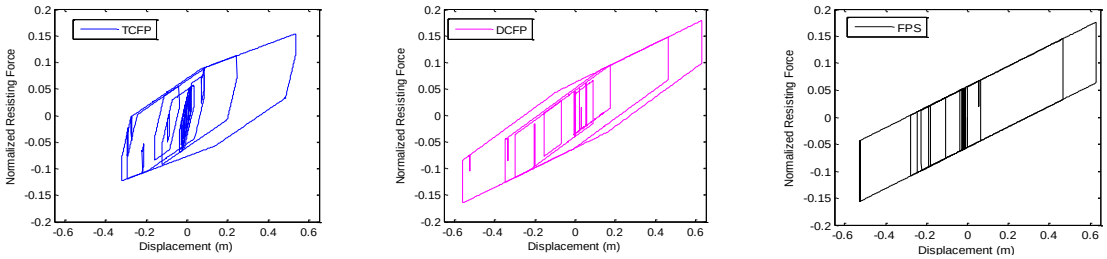

Fig. 11 Hysteresis loop of: (a) TCFP (b) DCFP; and (c) FPS bearings subjected to the Duzce Earthquake (T_s=0.3 s, T_{eff}=4 s, ξ_{eff}=15%)

Then records were scaled to MCE hazard level. The site chosen was located in San Francisco, with S_{MS}=1.5 g, where high earthquake hazard is expected. According to ASCE7-10, S_{Ms} defines as the MCE, 5 percent damped, spectral response acceleration parameter at short period.

In this study, superstructure period (T_s), effective period (T_{eff}) and effective damping (ξ_{eff}) were considered variable parameters, and an attempt was made to examine the effect of the variation in these parameters on the peak values of the seismic responses of the isolated structure such as base shear and bearing displacement. Average peak value for seven records was considered to compare responses for different isolation systems to find out the most efficient seismic performance and the superior behavior of each one in comparison to the others.

6.1 Hysteretic behavior and time history responses

Figs. 11-13 show the hysteretic loops of the isolator (normalized with the vertical load of the structure) subjected to Duzce, Kobe and Elcentro earthquakes for three different types of isolation system. When unloading begins, because of the presence of inner sliding surfaces with very small radii in the TCFP system, it occurs in a very sharp trade. The sharp unloading curve for the TCFP systems makes the hysteretic loops much squattier than the hysteretic loops for the DCFP and FPS, leading to have smaller displacements in the former isolated system.

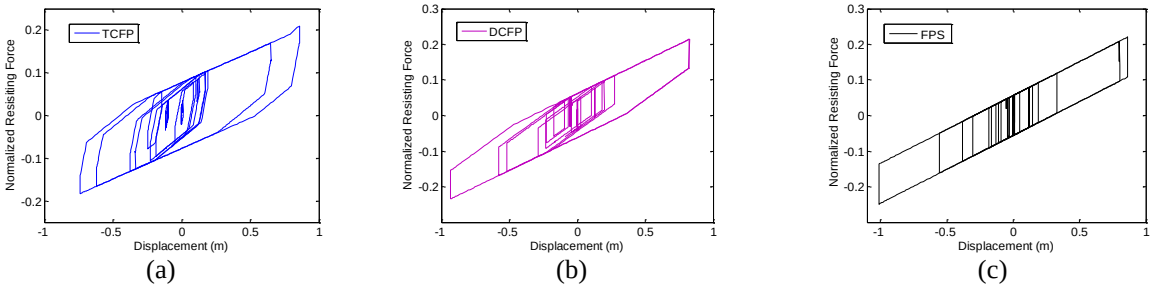

Fig. 12 Hysteresis loop of: (a) TCFP (b) DCFP and (c) FPS bearings subjected to the Kobe Earthquake (T_s=0.3 s, T_{eff}=4 s, ξ_{eff}=15%)

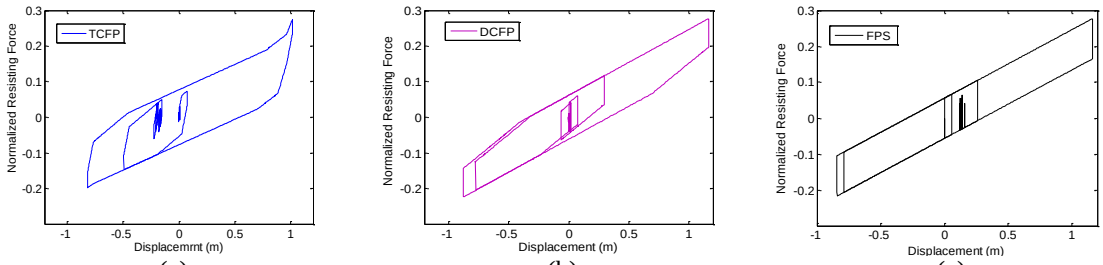

Fig.13 Hysteresis loop of: (a) TCFP (b) DCFP; and (c) FPS bearings subjected to the Elcentro Earthquake (T_s=0.3 s, T_{eff}=4 s, ξ_{eff}=15%)

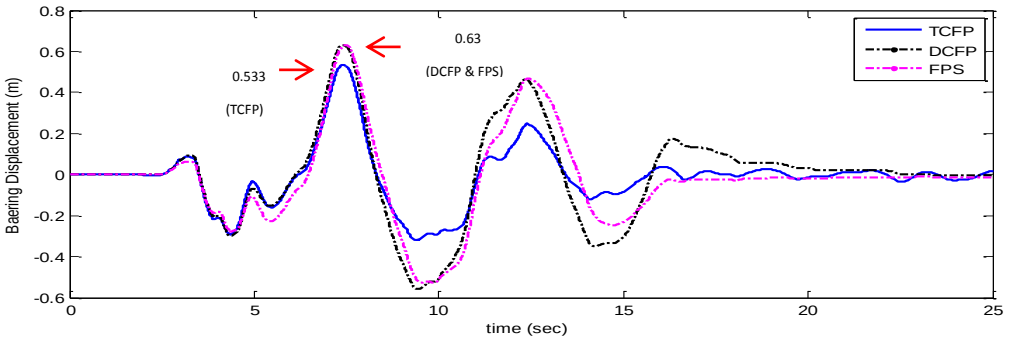

Fig. 14 Time variation of bearing displacements under Duzce Earthquake (T_s=0.3 s, T_{eff}=4 s, ξ_{eff}=15%)

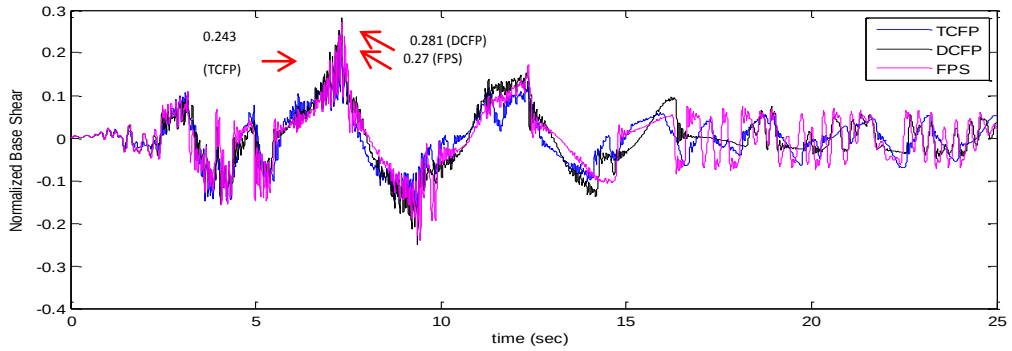

Fig. 15 Time variation of normalized base shear under Duzce Earthquake (T_s=0.3 s, T_{eff}=4 s, ξ_{eff}=15%)

Figs. 14 and 15 present the time variation of bearing displacement and normalized base shear of the isolated structure subjected to Duzce earthquake. Fig. 14 depicts that the bearing displacement for the structure mounted on TCFP is less than that of the other studied systems and the peak values of the variable for the structure equipped with DCFP and FPS are very close to each other. Also, the base shear of the structure equipped with different isolators illustrates the reduction in the base shear of the structure when the TCFP system is used (Fig. 15). The peak base shear value obtained from each isolator is illustrated in the figures.

6.2 Superstructure period

Fig. 16 depicts the effect of the superstructure period (T_s) on the peak bearing displacement of the isolators. The average bearing displacement under seven records indicates that the change in the superstructure period has negligible effect on the peak bearing displacement. The maximum values obtained from the DCFP and FPS systems are very close to each other and greater than those obtained from the TCFP, except in the superstructure with T_{eff}=3 s, where the displacement obtained from the three different isolator types coincided. Figs. 16(a)-16(c) show that when the effective isolation period decreases, the bearing displacement value is reduced. This happens because the decrease in effective isolation period is due to an increase in the effective stiffness which leads to a reduction in bearing displacements. The maximum difference for the DCFP and FPS with T_{eff}=5 sec is estimated to be 11.2 and 10.1 percent greater than the TCFP system, respectively. To investigate the precision of responses, the mean value of the bearing displacement plus standard deviation for seven records is added to each figure. The maximum differences between mean values and mean values plus standard deviation assuming T_{eff}=3 sec are 34.77%, 40.35%, and 44.16% for TCFP, DCFP and FPS isolators, respectively. These figures show when the effective isolation period increases, these differences between mean values and mean values plus standard deviation decrease. These differences are 16% for TCFP, 16% for DCFP, and 16.3% for FPS in T_{eff}=5 s, as well. In addition, the standard deviations demonstrate the accuracy of the selected records as well as the obtained results.

Fig. 17 shows the mean peak base shear subjected to the seven near field earthquake motions varying with superstructure period. This figure clearly indicates that a base-isolated structure mounted on the TCFP bearing has smaller base shear compared to that obtained from the other isolators for all periods. The maximum difference of mean peak base shear between the TCFP isolator and the DCFP and FPS isolators is 21.3 and 20.5 percent, for T_{eff}=5 sec, respectively. Although the mean base shear value differs for variation of superstructure period, there is a little difference in the base shear decrease value and it can be noted that the difference is independent of the superstructure period.

Also, Figs. 17(a)-17(c) demonstrate that a decrease in the effective isolation period leads to an increase in the base shear value. Because the decrease in the effective isolation period is due to an enhancement in the effective stiffness which leads to increase in the base shear exerted on the structure.

The maximum differences between mean values and mean values plus standard deviation for base shear are slightly more than these differences for bearing displacements. The maximum are 52.8%, 54.4%, and 54.5% for TCFP, DCFP and FPS in T_{eff}=3 s, respectively. As noted before, there is a reduction in these differences when effective isolation period increases. The differences are 43.73% for TCFP, 38.45% for DCFP, and 38.33% for FPS in T_{eff}=5 s.

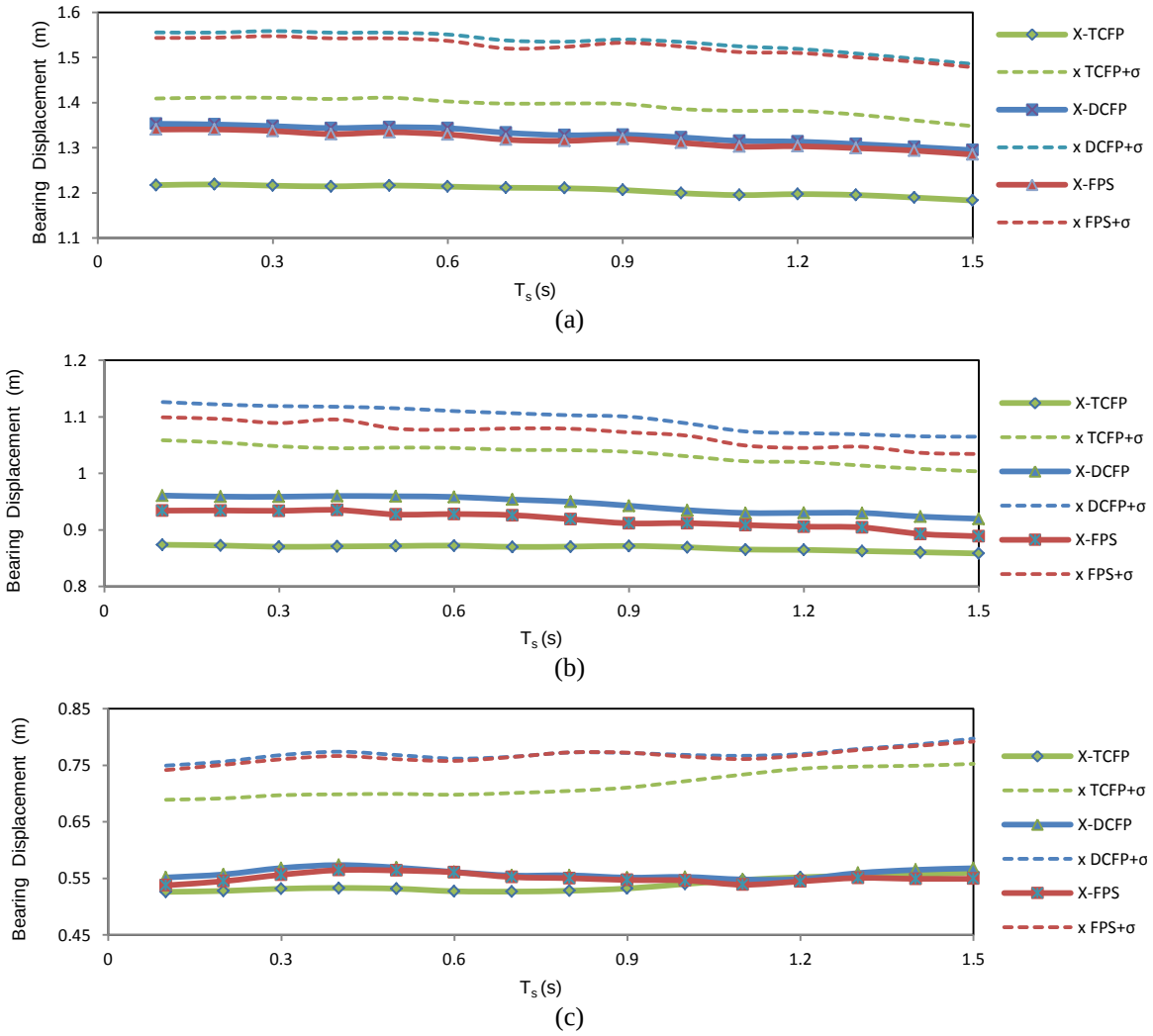

Fig. 16 Variation of peak bearing displacement for TCFP, DCFP, FPS isolators (a) (T_{eff}=5 s, ξ_{eff}=15%), (b) (T_{eff}=4 s, ξ_{eff}=15%) and (c) (T_{eff}=3 s, ξ_{eff}=15%)

6.3 Effective isolation period

Fig. 18(a) illustrates the impact of effective isolation period (T_{eff}) on the normalized base shear of the three base-isolated systems. The range of effective isolation period (T_{eff}) is selected due to the practical range of isolators' period and previous investigations (Pant *et al.* 2013). This figure confirms that an isolated structure using TCFP bearing is capable of reducing the base shear more effectively than structures isolated with the DCFP and FPS isolators. The maximum difference is seen in T_{eff}=5 s and has been estimated 21.3 percent.

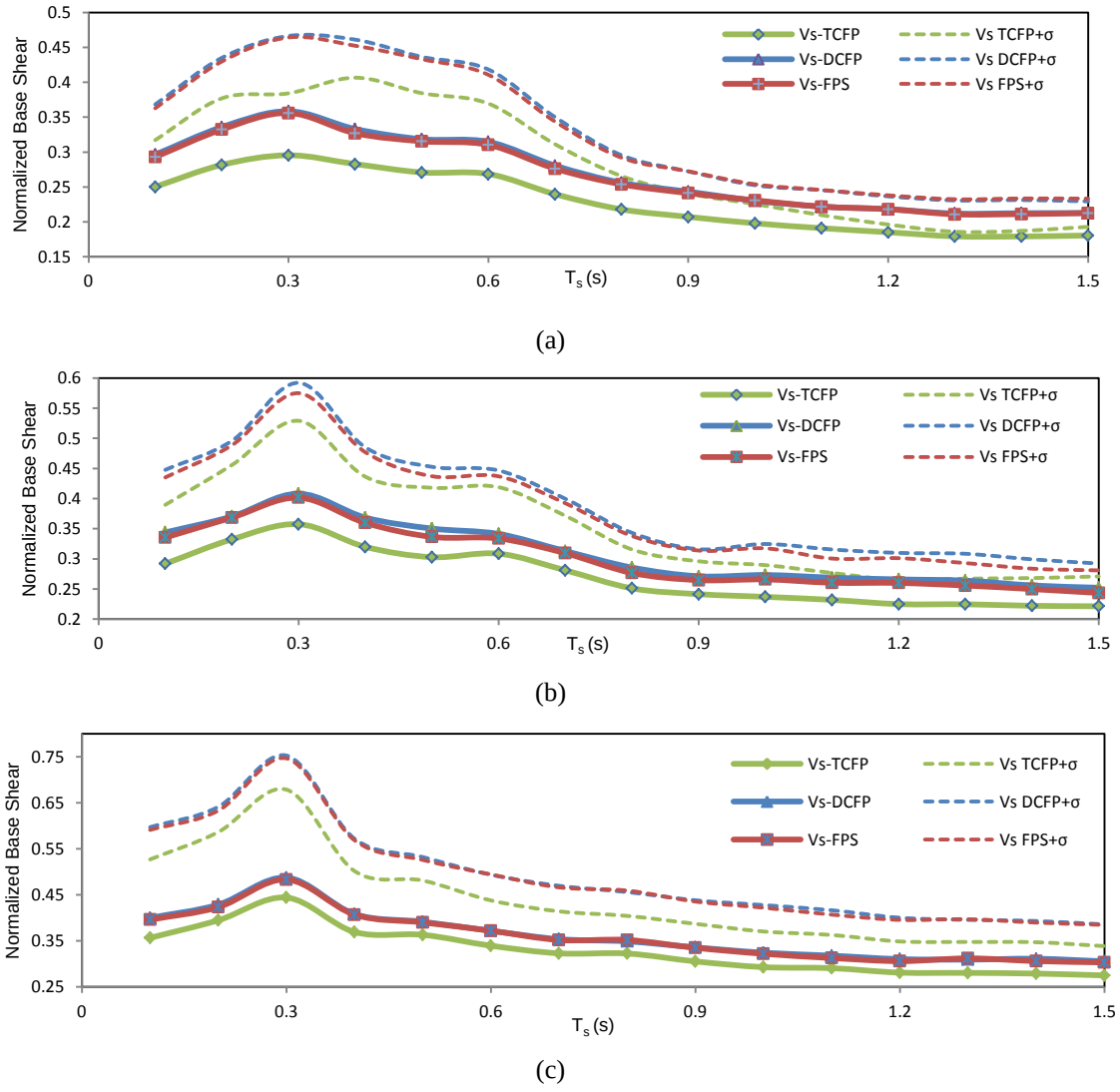

Fig. 17 Variation of normalized base shear for TCFP, DCFP, FPS isolators (a) (T_{eff}=5 s, ξ_{eff}=15%), (b) (T_{eff}=4 s, ξ_{eff}=15%) and (c) (T_{eff}=3 s, ξ_{eff}=15%)

Fig. 18(b) shows the influence of the effective isolation period on the peak bearing displacement. The figure demonstrates that for higher effective isolation period, the difference in bearing displacement increases. The maximum difference has been calculated at about 10.8 percent for T_{eff}=5 s.

As Figs. 18(a) and 18(b) illustrate, when the effective isolation period increases the differences in base shear and bearing displacement will also increase. The main reason can be explained by the shape of the backbone curve of TCFP compared to that of other isolators (Fig. 7). As noted before, the TCFP isolator has a hardening sliding section in the backbone curve (named IV and V), which is the main difference between its curve and that of other isolators. According to the Fig. 7, for an

isolation system with T_{eff}=4 s, the stiffening region or section IV begins when the bearing displacement reaches 0.78 m. Therefore, more differences in responses would be expected after entrance into this sliding regime. The bearing displacement in Fig. 18(b) depicts that near T_{eff}=4 s the TCFP will enter sliding regime IV, where the distinction between the different isolators enhances.

The sharp unloading pattern discussed in section 6.1 is another reason for the differences in responses between the TCFP and the other systems. As seen before, there is no noticeable difference in results for the DCFP and FPS systems in this hazard level. It is expected that the results of DCFP and FPS bearings could be different for lower hazard levels.

Furthermore, the mean values plus the standard deviations added to figure show that the accuracy of the obtained results.

6.3 Effective isolation damping

Fig. 19(a) depicts the influence of the isolator's effective damping on base shear. According to this diagram, the maximum base shear difference happens with lower effective damping values. The maximum distinction is 26.8 percent, for ξ_{eff}=10%.

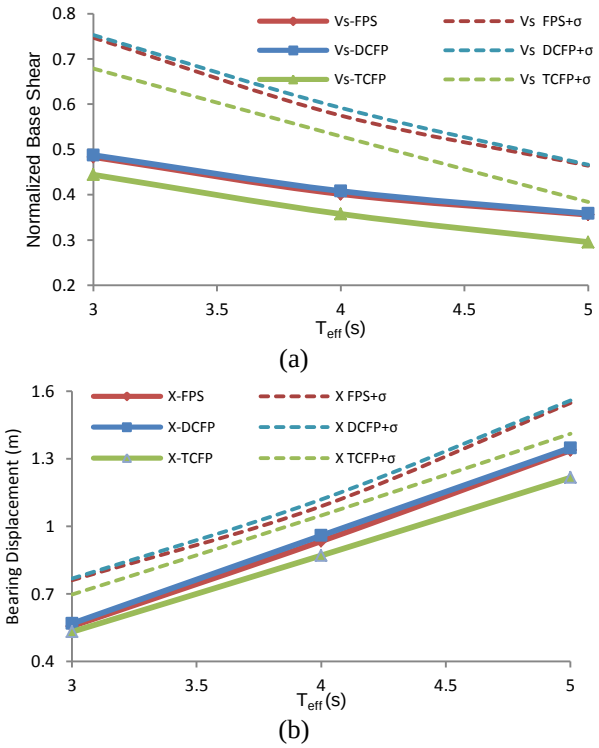

Fig. 18 (a) Variation of normalized base shear for TCFP, DCFP, FPS isolators (T_s=0.3 s, ξ_{eff}=15%) and (b) Variation of bearing displacement for TCFP, DCFP, FPS isolators (T_s=0.3 s, ξ_{eff}=15%)

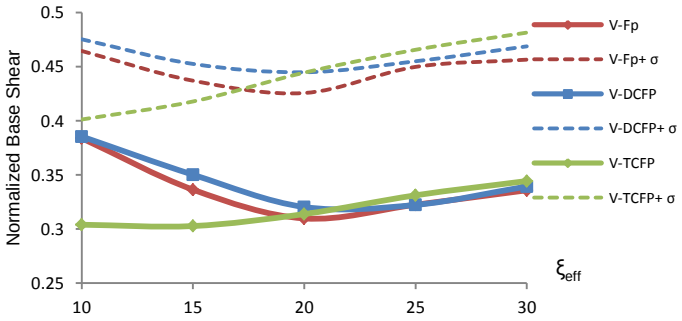

(a)

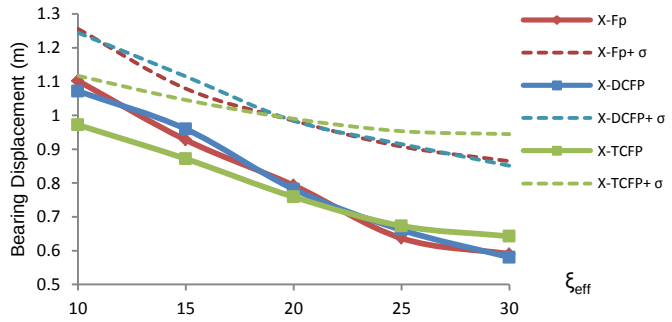

(b)

Fig. 19 (a) Variation of normalized base shear for TCFP, DCFP, and FPS isolators (T_{eff}=4 s, T_s=0.5 s) and (b) Variation of bearing displacement for TCFP, DCFP, and FPS isolators (T_{eff}=4 s, T_s=0.5 s)

Fig. 19(b) indicates that the impact of isolator effective damping on bearing displacement is considerable for lower effective damping values as well. This figure demonstrates that a system with TCFP isolator undergoes smaller displacements that appraised about 13.4 percent for ξ_{eff}=10%. This figure also shows that increase in damping values nullifies the superiority of TCFP.

These figures show that for effective damping values lower than 20%, the difference is remarkable. It can be seen that an increase in the effective damping of the isolator causes a decrease in the differences between the responses obtained from the three isolators. Therefore, the advantages of using TCFP bearings over DCFP and FPS bearings would be negligible in these cases. As it was mentioned, the main reason for this observation can be found in the backbone curve of TCFP (Fig. 7). According to Fig. 7, sliding section IV begins when displacement reaches 0.78 m. In diagram 19(b), this displacement reached at an effective damping of 20%. Therefore, it is obvious that the increase in damping practically prevents TCFP to experience stiffening sections IV and V. Thus, the differences in responses are more remarkable with lower effective damping, where TCFP experiences all sliding regimes.

As discussed in section 6.1, the sharp unloading pattern due to squattier hysteretic loops for TCFP is another reason for the differences in responses. It means that for the same area the TCFP system has a smaller width that leads to smaller displacement. As seen before, there is no noticeable difference in results for DCFP and FPS systems in this hazard level.

Moreover, the mean values plus standard deviations which show the precision of results are added to the figures. The maximum differences between mean values and mean plus standard

deviation for base shear are estimated 41.63% for TCFP, 41.88% for DCFP, and 39.5% for FPS in ξ_{eff}=25%.

7. Conclusions

In this study, the seismic responses of an idealized two dimensional SDOF building mounted on different types of friction isolators: TCFP, DCFP, and FPS and subjected to seven MCE scaled near field earthquake motions were investigated. The superstructure period, the effective isolation period and damping were selected as the variable parameters of the base-isolated structure, and attempt was made to compare the responses of these isolated structures. From the results of the present study, the following conclusions were summarized:

- The results generally show that a structure with TCFP isolator will experience less base shear and bearing displacement in comparison with a system employing DCFP or FPS bearings. Also, there is no noticeable difference in results for DCFP and FPS systems in the investigated earthquake hazard level. However, it is expected that this difference could be significant for lower earthquake hazard levels.
- Changes in superstructure period have little effect on base shear and bearing displacement. The base shear for TCFP was estimated at 21.3 and 20.5 percent less than that obtained from the DCFP and FPS systems. Bearing displacement difference obtained from TCFP was about 11.2 and 10.1 percent less than that obtained from DCFP and FPS for ξ_{eff}=15%, respectively.
- For higher effective isolation periods, the difference in responses obtained from the three isolators becomes considerable. The maximum difference between the results obtained from TCFP and DCFP and FPS for base shear and bearing displacement were calculated 21.3 and 10.8 percent, respectively, while T_{eff}=5 s.
- An increase in the effective damping of isolator causes a reduction in the response differences between the three isolators. The maximum distinction for base shear and bearing displacement is 26.8 and 13.4 percent for ξ_{eff}=10%, respectively.

References

Almazan, J.L., De la llera, J.C. and Inaudi, J.A. (1998), "Modeling aspects of structures isolated with the frictional pendulum system", *Earthq. Eng. Struct. D.*, **27**(80), 845-867.

ASCE7-10 (2010), *Minimum design loads for building and other structures*, American Society of Civil Engineers, USA.

Bagheri, M. and Khoshnoudian, F. (2014), "The effect of impact with adjacent structure on seismic behavior of base-isolated buildings with DCFP bearings", *Struct. Eng. Mech.*, **51**(2), 277-297.

Baker, J.W. (2007), "Quantitative classification of near-fault ground motions using wavelet analysis", *B. Seismol. Soc. Am.*, **97(**5), 1486-1501.

Becker, T.C. and Mahin, S.A. (2011), "Experimental and analytical study of the bi-directional behavior of the triple friction pendulum isolator", *Earthq. Eng. Struct. D.*, Published online in Wiley online Library, DOI:10.1002/eqe.1133.

Becker, T.C. and Mahin, S.A. (2013), "Approximating peak responses in seismically isolated buildings using generalized modal analysis", *Earthq. Eng. Struct. D.*, Published online in Wiley online Library, DOI:10.1002/eqe.2299.

Constantinou, M.C., Kalpakidis, I., Filiatrault, A. and Ecker Lay, R.A. (2011), *LRFD-based analysis and*

design procedures for bridge bearings and seisemic isolation, Technical Report MCEER-11-0004, State University of New York at Buffalo, Buffalo, New York, USA.

Fadi, F. and Constantinou, M.C. (2009), "Evaluation of simplified methods for analysis for structures with triple friction pendulum isolators", *Earthq. Eng. Struct. D.*, **39**, 5-22.

FEMA 695 (2009), *Quantification of building seismic performance factors*, Applied Technology Council, California, USA.

Fenz, D.M. and Constantinou, M.C. (2006), "Behavior of the double concave friction pendulum bearing", *Earthq. Eng. Struct. D.*, **35**(11), 1403-1424.

Fenz, D.M. and Constantinou, M.C. (2007a), "Spherical sliding isolation bearings with adaptive behavior: Theory", *Earthq. Eng. Struct. D.*, **37**(2), 163-183.

Fenz, D.M. and Constantinou, M.C. (2007b), "Spherical sliding isolation bearings with adaptive behavior: Experimental verification", *Earthq. Eng. Struct. D.*, **37**(2), 185-205.

Fenz, D.M. and Constantinou, M.C. (2008a), *Mechanical behavior of multi-spherical sliding bearings*, Technical Report MCEER-08-0007, State University of New York at Buffalo, Buffalo, New York, USA.

Fenz, D.M. and Constantinou, M.C. (2008b), "Modeling triple friction pendulum bearings for response-history analysis", *Earthq. Spectra*, **24**(4), 1011-1028.

Fenz, D.M. and Constantinou, M.C. (2008c), *Development, implementation and verification of dynamic analysis models for multi-spherical sliding bearings*, Technical Report MCEER-08-0018, Multidisciplinary Center for Earthquake Engineering Research, State University of New York at Buffalo, Buffalo, New York, USA.

Gueraud, R., Noel-leroux, J.P., Livolant, M. and Michalopoulos, A.P. (1985), "Seismic isolation using sliding elastomer bearing pads", *Nuclear Eng. Des*., **84**(3), 363-377.

Kim, Y.S. and Yun, C.B. (2007), "Seismic response characteristics of bridges using double concave friction pendulum bearings with tri-linear behavior", *Eng. Struct.*, **29**(11), 3082-3093.

Khoshnoudian, F. and Hemmati, A. (2011), "Seismic response of base-isolated structures using DCFP bearings wih tri-linear and bi-linear behaviors", *Proceedings of the 12th Asia-Pacific Conference on Structural Engineering and Construction*. *Procedia Engineering*.

Khoshnoudian, F, and Rabie, M. (2011), "Response of multistory friction pendulum base-isolated buildings including the vertical component of earthquakes", *Can. J. Civil Eng.*, **38**, 1045-1059.

Khoshnoudian, F. and Rabie, M. (2010), "Earthquake response of double concave friction pendulum base-isolated structures considering vertical component of earthquake", *Adv. Struct. Eng.*, **13** (1). 1-14.

Loghman V., Khosnoudian F. and Banazadeh M. (2013), "Effects of vertical component of earthquake on seismic responses of triple concave friction pendulum base-isolated structures", *J. Vib. Control.,* DOI: 10.1177/1077546313503359.

Malekzadeh, M. and Taghikhany, T. (2010), "Adaptive behavior of double concave friction pendulum bearing and its advantages over friction pendulum systems", *Scientla Iranica*, **17**(2), 81-88.

Matsagar, V.A. and Jangid, R.S. (2004), "Influence of isolator characteristics on the response of base-isolated structures", *Eng. Struct*., **26**(12), 1735-1749.

Morgan, T.A. and Mahin, S.A. (2011), *The use of base-isolation system to achieve complex seismic performance objectives*, Peer Report 2011/06, Pacific Earthquake Engineering Research Center, College of Engineering University of California, Berkeley, USA.

Mostaghel, N. and Khodaverdian, M. (1987), "Dynamics of resilient-friction base isolator (R-FBI)", *Earthq. Eng. Struct. D.*, **15**(3), 379-390.

Mostaghel, N. and Tanbakuchi, J. (1983), "Response of sliding structures to earthquake support motion", *Earthq. Eng. Struct. D.*, **11**(6), 729-748.

Panchal, V.R. and Jangid, R.S. (2008), "Seismic behavior of variable frequency pendulum isolator", *Earthq. Eng. Eng. Vib*., **7**,193-205.

Panchal, V.R. and Jangid, R.S. (2011), "Performance of variable friction pendulum system for torsionally coupled structures", *J. Vib. Contol.,* **18**(3), 323-343.

Pant, D.R., Constantinou, M.C. and Wijeyewickrema, A.C. (2013), "Re-evaluation of equivalent lateral force procedure for prediction of displacement demand in seismically isolated structures", *Eng. Struct.*, **52**, 455-465.

Scheller, J. and Constantinou, M.C. (1999), *Response history analysis of structures with seismic isolation and energy dissipation systems: Verification examples for program SAP2000*, Technical Report No. MCEER 99-02, Multidisciplinary Center for Earthquake Engineering Research, Buffalo, New York, USA.

Tajammolian, H., Khoshnoudian, F., Talaee, S. and Loghman, V. (2014) "The effects of peak ground velocity of near-field ground motions on the seismic responses of base-isolated structures mounted on friction isolators", *Earthq. Struct.*, **7**(6), 1159-1282.

Tsai, C.S., Chen, B.J., Pong, W.S. and Chiang, T.C. (2004), "Interactive behavior of structures with multiple friction pendulum isolation system and unbounded foundations", *Adv. Struct. Eng*., **7**(6), 539-551.

Tsai, C.S., Chiang, T.C. and Chen, B.J. (2005), "Experimental evaluation of piece wise exact solution for predicting seismic responses of spherical sliding type isolated structures", *Earthq. Eng. Struct. D.*, **34**(9), 1027-1046.

Yang, Y.B., Lee, T.Y. and Tsai, I.C. (1990), "Response of multi-degree-of-freedom structures with sliding supports", *Earthq. Eng. Struct. D.*, **19**(5), 739-752.

Zayas, V.A., Low, S.S. and Mahin, S.A. (1987), *The FPS earthquake resisting system*, Experimental report No. UCB/EERC 87/01, EERC, University of California, Berkeley, USA.

Zayas, V.A., Low, S.S. and Mahin, S.A. (1990), "A simple pendulum technique for achieving seismic isolation", *Earthq. Spectra*, **6**(2), 317-333.

CC